

CrossMark
click for updatesCite this: *Anal. Methods*, 2015, 7, 6089

Highly sensitive simultaneous electrochemical determination of hydroquinone, catechol and resorcinol based on carbon dot/reduced graphene oxide composite modified electrodes†

Wuxiang Zhang,^a Jianzhong Zheng,^a Zhongqiu Lin,^a Ling Zhong,^a Jiangu Shi,^a Chan Wei,^a Hanqiang Zhang,^a Aiyao Hao^b and Shirong Hu^{*ab}

In this work, a simple and highly sensitive electrochemical method was developed for the simultaneous detection of hydroquinone (HQ), catechol (CC) and resorcinol (RC) based on a carbon dot/reduced graphene oxide composite on a glassy carbon electrode (GCE). The electron communication between reduced graphene oxide (r-GO) and CDs can be further strengthened via hydrogen bonding and π - π stacking forces. The electrochemical behavior of the CD/r-GO/GCE sensor toward HQ, CC and RC was probed by cyclic voltammetry (CV) and differential pulse voltammetry (DPV). The results showed that the calibration curves were in the range of 0.5 to 1000 μM , 1.0 to 950 μM and 5.0 to 600 μM , respectively. The detection limits for HQ, CC and RC were 0.17 μM , 0.28 μM and 1.0 μM (S/N = 3), respectively. Moreover, the sensor has been successfully applied in detecting tap water, river water and industrial sewage.

Received 31st March 2015

Accepted 15th June 2015

DOI: 10.1039/c5ay00848d

www.rsc.org/methods

1. Introduction

Dihydroxybenzene isomers, hydroquinone (HQ), catechol (CC) and resorcinol (RC), are derived from a wealth of sources, including agriculture, factory discharges, wastewater treatment plants and other related industries.¹⁻³ Owing to their low degradation in the environment and high toxicity to the environment and humans, the US Environmental Protection Agency (EPA) and the European Union have classified dihydroxybenzene isomers as environmental pollutants.⁴ Therefore, simultaneous determination of dihydroxybenzene isomers has become a hot topic for scientists.⁵ Until now, chromatography,^{6,7} spectrophotometry⁸ and electrochemical methods have been designed for the simultaneous detection of dihydroxybenzene isomers. Among these methods, electrochemical detection is the most promising technology because of many intrinsic advantages such as rapid response, high sensitivity and low cost.^{9,10} However, the key problem in simultaneously detecting HQ, CC and RC here is the interference with each other and their peak currents are overlapped at conventional electrodes.¹¹ In this context, it is particularly urgent to explore a novel electrode material to modify glassy carbon electrodes

(GCEs) for simultaneous determination of dihydroxybenzene isomers.

Graphene, which is a single atomic sheet of conjugated sp^2 carbon atoms, has been extensively studied due to its excellent characteristics with large surface structure, good mechanical strength, high electronic conductivity and chemical stability.¹²⁻¹⁵ Moreover, many potential applications and unique properties of graphene can be realized by its integration into more complex assemblies. The synergetic effect not only exhibits its excellent charge transport rate, but also reduces graphene-supported hybrid material interfacial defects.¹⁶⁻¹⁹ Notably, many graphene-based composite chemicals have been developed for the detection of dihydroxybenzene isomers, including cadmium sulphide/reduced graphene oxide nanocomposites,²⁰ gold-graphene nanocomposites,²¹ reduced graphene oxide-multiwall carbon nanotubes,²² and tungsten sulfide-graphene nanocomposites.²³ All these studies indicated that graphene with composite nanomaterials could efficiently improve the performance of sensors. In order to enrich the potential applications, doping of other materials into graphene is the efficient way to enhance the electrochemical effects. Carbon dots (CDs), as a new class of “zero-dimensional” carbon materials, have recently attracted much attention for a variety of purposes and applications, especially for their potential applications in fluorescence, biosensors and imaging.²⁴⁻²⁷ Compared with conventional semiconductor quantum dots, CDs have the advantage in terms of biocompatibility, cytotoxicity and conductivity.^{28,29} The existence of sp^2 (graphitic) π bonds endows it with better charge-charge transport and

^aCollege of Chemistry and Environment, Minnan Normal University, Zhangzhou 363000, P. R. China. E-mail: Hushirong6666@163.com; Fax: +86 596 2528075; Tel: +86 596 2528075

^bSchool of Chemistry and Chemical Engineering, Shandong University, Jinan 250100, P. R. China

† Electronic supplementary information (ESI) available. See DOI: 10.1039/c5ay00848d

oxidation–reduction performance.^{30,31} Thus, nowadays, developing a novel CD based material is a strong challenging goal for the determination of dihydroxybenzene isomers. So we synthesized CDs by the method of reflux and applied carbon dot/reduced graphene oxide composites in electrochemical techniques for the determination of dihydroxybenzene isomers.

In this work, a novel sensor based on carbon dot/reduced graphene oxide (CD/r-GO) was constructed to detect HQ, CC and RC for the first time. The peak oxidation potentials of the dihydroxybenzene isomers are separated by differential pulse voltammetry (DPV). The calibration curves of HQ, CC and RC were obtained in the range of 0.5 to 1000 μM , 1.0 to 950 μM and 5.0 to 600 μM , respectively and the low limits of detection for HQ, CC and RC were 0.17 μM , 0.28 μM and 1.0 μM ($S/N = 3$). Furthermore, the CD/r-GO modified electrode has been applied for the simultaneous determination of HQ, CC and RC in practical water samples.

2. Experimental

2.1. Reagents and apparatus

Citric acid, sodium hydroxide, sodium borohydride and phosphate buffer solution were purchased from Sinopharm Chemical Reagent Co., Ltd. Hydroquinone, catechol and resorcinol were obtained from Xilong Chemical Co., Ltd. All reagents were analytical grade reagents. All chemicals and solvents were used as received. All aqueous solutions were prepared using ultra-pure water (18 $\text{M}\Omega$ cm) from a Milli-Q system (Millipore). Scanning electron microscopy (SEM) was conducted on a JEM-6010La (JEOL Japan) operating at 20 kV. Transmission electron microscopy (TEM) was performed on a FEI Tecnai G20 electron microscope operating at 300 kV (FEI Company, USA). The surface topography was observed with an Atomic Force Microscope (CSPM5500, China). UV-vis spectroscopy was carried out by using a UV-1800PC spectrophotometer (Shanghai Mapada Instruments Co., Ltd, China). Fourier transform infrared (FT-IR) spectroscopy was carried out on a Thermo NICOLET iS 10 (Thermo Fisher Scientific, America), the spectrophotometer operating between 500 cm^{-1} and 4000 cm^{-1} . Fluorescence spectra were obtained by using a Varian Cary Eclipse fluorescence spectrophotometer (Agilent Technologies, America). Electrochemical measurements were performed on a CHI660E electrochemical workstation. A glassy carbon electrode was used as the working electrode (CHI104). An Ag/AgCl electrode and platinum wire were used as reference and auxiliary electrodes, respectively.

2.2. Synthesis of carbon dot/reduced graphene oxide materials

Carbon dots (CDs) were synthesized by reflux heating 2.0 g citric acid and 10 mL distilled water in a 50 mL round-bottom flask at 200 ± 5 $^{\circ}\text{C}$ under magnetic stirring until yellow-black CDs were produced. Lastly, the CDs were dialyzed for 24 h with dialysis membranes of 1000 cutoffs and diluted in a 50.00 mL volumetric flask with water, then stored at 4 $^{\circ}\text{C}$ ready for use. Graphene oxide (GO) was synthesized by the oxidation of

graphite using the Hummers' method.³² The CD/r-GO was fabricated as follows: first, 4.0 mg of the obtained dry GO was ultrasonically redispersed into 20.00 mL deionized water, and then 2.00 mL of the as-obtained CDs was dissolved in the obtained dispersion for 20 min by sonication in a water bath (KQ2200DE, 40 kHz). The suspension was moved to a 50 mL round-bottom flask under mechanical stirring. After that, 2.0 mg sodium borohydride was added into the suspension when the suspension was heated up to 80 $^{\circ}\text{C}$ and maintained at this temperature for 2 hours. The CD/r-GO was thus obtained.

2.3. Modification of electrodes

Alumina powders of different sizes (1.0, 0.3 and 0.05 μm) were used to polish the GCE before use. The as-synthesized material (1.0 mg) was dispersed in 1 mL of chitosan solution (0.5 wt%) by ultrasonication to enhance the tackiness and selectivity of the electrode.³³ Then, 8.0 μL of the suspension was added dropwise on the surface of the GCE and dried in an oven at 60 $^{\circ}\text{C}$ for 20 min.

3. Results and discussion

3.1. Characterization of GO, CDs and CD/r-GO composite

The surface morphologies of GO and CD/r-GO were investigated by scanning electron microscopy (SEM). As shown in Fig. 1A, the morphology of the GO layer resembles a thin wrinkled paper.³⁴ The transmission electron microscopy (TEM) image of the obtained CDs in Fig. 1B shows that these small CDs were well dispersed with a diameter of about 2.32 ± 0.8 nm, which was consistent with previous reports.³⁵ The inset in Fig. 1B shows the particle size distribution. It can be observed in Fig. 1C that the crumpled graphene sheets were randomly aggregated and overlapped with each other, which is characteristic of CD/r-GO.

An atomic force microscope (AFM) is a suitable instrument to evaluate the topography of materials. The AFM images of GO/GCE (Fig. 2A), CD/GCE (Fig. 2B) and CD/r-GO/GCE (Fig. 2C) were used to explain the structures of the modified electrodes. It is observed that the surface of the GO/GCE was a hillock-like surface morphology and relatively smooth with an average roughness of 0.85 nm. The average roughness of the regular tapered convex surface of the CD/GCE was 2.34 nm. The irregular spinous islands and adjacent peaks on the CD/r-GO/GCE with an average roughness of 14.30 nm indicated that the surface morphology changed the roughness of each surface, and the GO, CDs and CD/r-GO had been successfully modified on the electrodes. The change mechanism of topographies may be as follows: in the reduction process of graphene oxide, the covalent bond and the layered structure were destroyed; r-GO in different sections of materials was mutually stacked and heaped. In addition, CDs attached between the r-GO layers could also increase the roughness of the composite.

The optical properties of CDs are shown in Fig. 3A. The obvious absorption features of the UV-vis absorption spectrum were at approximately 226 nm and 275 nm, which were ascribed to the π - π^* transition of C=C in amorphous carbon systems.³⁶ The typical characteristic peaks of GO are at 230 nm and

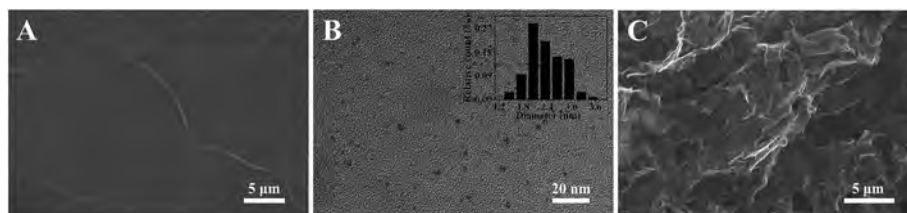


Fig. 1 SEM images of GO (A), TEM images of CDs. Inset: size distribution of CDs (B) and SEM images of CD/r-GO (C).

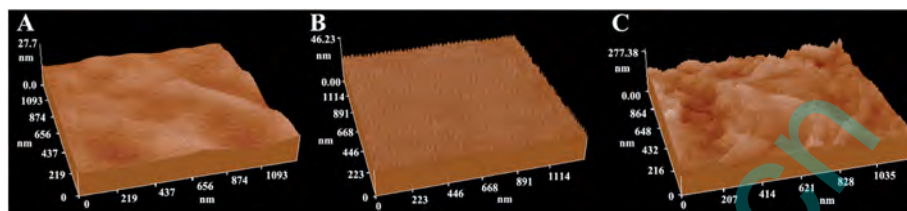


Fig. 2 AFM images of GO/GCE (A), CD/GCE (B) and CD/r-GO/GCE (C).

300 nm, consistent with the previous report.³⁷ In contrast, there is a weak absorption peak of the CD/r-GO at 260 nm ascribable to the CDs that reacted with GO to form CD/r-GO. The photoluminescence spectra in Fig. 3A suggest that the excitation wavelength of the emission spectrum was 446 nm and the emission wavelength of the excitation spectrum was 530 nm. The photoluminescence properties of CDs are mainly attributed to size differences.³⁸ The functional groups were further characterized by FT-IR spectroscopy. As seen from the comparison in Fig. 3B, due to the existence of negatively charged carboxyl and hydroxyl groups on the surface of CDs, the peaks at 1713 cm^{-1} , 1403 cm^{-1} and 1202 cm^{-1} were assigned to the carbonyl/benzodiazepine characteristic vibrations of C=O, C=C and C-OH (phenolic) stretching bonds, respectively. The FT-IR peaks at 3400 and 3500 cm^{-1} are attributed to the stretching vibrations of O-H. The GO peak was at 2900 cm^{-1} , which is assigned to C-H bonds of sp^3 hybrid carbon, while the peak at 1050–1465 cm^{-1} indicates the existence of epoxy, C-O and C=C bonds.³⁹ It was obviously seen that the peak intensities of C-O, C=C and C=O were much weaker in CD/r-GO materials, which indicates that most of the oxygen-containing groups were removed after the reaction and the composite CD/r-GO was achieved.

3.2. Electrochemical behavior of dihydroxybenzene isomers

Cyclic voltammetry (CV) and electrochemical impedance spectroscopy (EIS) were used to exploit the signal amplification capability of the different electrodes in a 1.0 mM $[\text{Fe}(\text{CN})_6]^{3-/4-}$ and 0.1 M KCl mixed solution, as shown in Fig. S1.† As can be seen from Fig. S1A,† the redox peaks of the GCE were the weakest. While at the CD/r-GO/GCE, the current of both anodic and cathodic peaks greatly increased due to the modification of CD/r-GO on the GCE, which may greatly accelerate the electron transfer rate.⁴⁰ Fig. S1B† shows the EIS spectra of different electrodes. On the bare GCE, the R_{et} value was 400 Ω . When r-GO was modified onto the GCE surface, the R_{et} value dramatically increased to about 1560 Ω , suggesting that r-GO acted as an insulating layer which caused difficulties during the interfacial electron transfer due to its disrupted sp^2 bonding networks.⁴¹ While on the CD/GCE, the R_{et} value decreased compared to the bare electrode, indicating that the CDs could accelerate the electron transfer rate. However, the R_{et} value increased to 1390 Ω on the CD/r-GO modified GCE. The R_{et} value increased obviously illustrating that the CDs were successfully functionalized on r-GO and the CD/r-GO modified GCE was obtained.

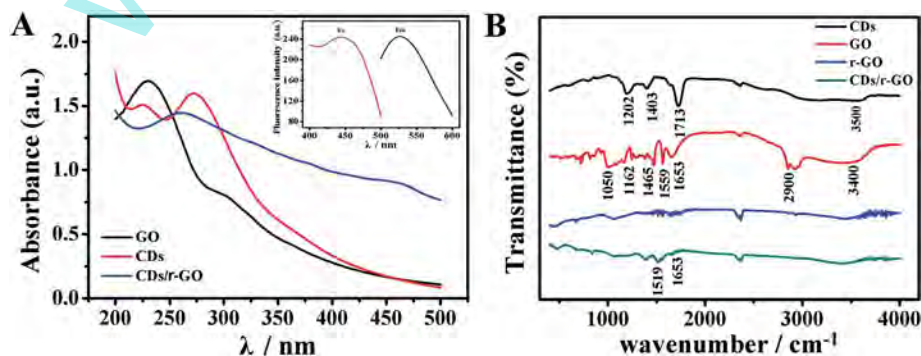


Fig. 3 (A) UV-vis absorption spectra (Abs) and fluorescence spectra (Ex, Em) of the CD intensity and (B) FT-IR spectra of CDs, GO, r-GO and CD/r-GO.

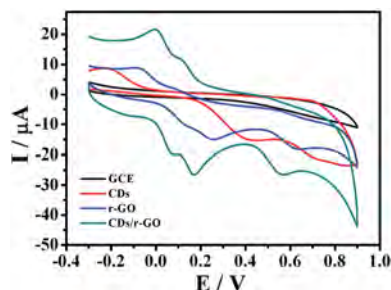


Fig. 4 Cyclic voltammograms of 0.2 mM HQ, CC and RC at the GCE, r-GO/GCE, CD/GCE and CD/r-GO/GCE.

The electrochemical properties of different electrodes of GCE, r-GO/GCE and CD/r-GO/GCE were studied in 0.1 M phosphate solutions. As illustrated in Fig. 4, the oxidation peak current of dihydroxybenzene isomers increased significantly for the CD/r-GO/GCE. A possible reaction mechanism was discussed. As the electron collectors and transporters, some unoxidized aromatic rings of r-GO would provide a selective interface by hydrogen bonds and rich delocalized π electrons. After chemical reduction of CDs and graphene oxide, the strong π - π stacking force, hydrogen bonding force and sp^2 and sp^3 hybrid structures could accumulate CDs around the r-GO layers. At the CD/r-GO/GCE, the proton-donating groups of HQ, CC and RC molecules facilitated the charge transport rate, which significantly enhanced the corresponding peak current and exhibited improved catalytic separation performance of the coexisting HQ, CC and RC.

3.3. Effects of scan rate and pH

In the following experiment, electrochemical behaviors of hydroquinone, catechol and resorcinol (CV of 0.2 mM dihydroxybenzene isomers on the CDs/r-GO/GCE) were studied at various scan rates. As the scan rate increases, the oxidation peak current increases linearly as well. The redox peak current was proportional to the scan rate in the range of 0.01 – 0.4 $V s^{-1}$, as shown in Fig. 5. Moreover, with the increase of the scan rate, the redox potential of HQ, CC and RC shifted positively. The oxidation peak current (I_{pa}) shows a linear relationship with the

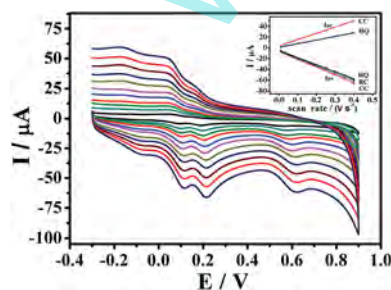


Fig. 5 CV of 0.2 mM HQ, CC and RC on the CD/r-GO/GCE at different scan rates (0.01, 0.03, 0.05, 0.075, 0.10, 0.15, 0.20, 0.25, 0.30, 0.35, and 0.40 $V s^{-1}$). Inset: the relationship of the redox peak current with the scan rate.

scan rate (ν) whose equation is $HQ I_{pa} (\mu A) = -131.62\nu (V s^{-1}) - 4.97$ ($R = 0.9969$) and $I_{pc} (\mu A) = 67.47\nu (V s^{-1}) + 1.04$ ($R = 0.9974$). For CC, $I_{pa} (\mu A) = -147.18\nu (V s^{-1}) - 6.28$ ($R = 0.9967$) and $I_{pc} (\mu A) = 116.27\nu (V s^{-1}) + 3.71$ ($R = 0.9961$). For RC, only an oxidation peak was observed, which proves once again that the oxidation process is a totally irreversible electrode process, and the linear regression equations of RC can be expressed as $I_{pa} (\mu A) = -136.33\nu (V s^{-1}) - 6.42$ ($R = 0.9963$), which indicated that the redox reactions of HQ, CC and RC on the CD/r-GO/GCE were typical adsorption-controlled processes.⁴²

The effect of the pH value on the CV response of 0.2 mM dihydroxybenzene isomers on the CDs/r-GO/GCE was investigated and is shown in Fig. S2.† The reduction potential shifted negatively and the peak current remained basically consistent as the pH value increased until it reaches 7.0. However, upon further increase of the pH value, the reduction peak current decreased. In order to reduce the over-potential and enhance the electron transfer rate, pH 7.0 of PBS solutions was chosen as the optimal value in this experiment.

3.4. Differential pulse voltammetry simultaneous determination of HQ, CC and RC

Simultaneous detection of HQ, CC and RC was performed on the CDs/r-GO/GCE in 0.1 M phosphate solutions. As illustrated in Fig. 6A, with the increase of the HQ concentrations in the presence of 0.2 mM CC and 0.2 mM RC, the anodic peak currents of HQ linearly increased ranging from 0.5 to 1000.0 μM , the equation being: $I_{pa} (\mu A) = -0.045C (\mu M) - 40.01$ ($R = 0.9964$). Similarly, as shown in Fig. 6B, keeping the concentration of HQ and RC constant (0.2 mM), the oxidation peak current increased linearly with increasing concentration of CC in the range of 1.0 to 950.0 μM , the equation: $I_{pa} (\mu A) = -0.058C (\mu M) - 23.90$ ($R = 0.9951$). From the DPVs of RC with different concentrations in the presence of 0.2 mM HQ and CC (Fig. 6C), the linear regression equation is calibrated as $I_{pa} (\mu A) = -0.031C (\mu M) - 17.78$ (5.0 to 600.0 μM , $R = 0.9973$). The detection limits ($S/N = 3$) for the detection of HQ, CC and RC were evaluated to be 0.17 μM , 0.28 μM and 1.0 μM . Thus, the selective and sensitive determination of HQ, CC and RC was achieved simultaneously at the CDs/r-GO/GCE. In addition, the peaks near -0.2 V have been shown in Fig. 6. The possible reason for the peaks near -0.2 V may be ascribed to the characteristic peak of the incomplete reduction of graphene oxide; the two close hydroxyl groups on carbon dehydrate to form a cycle and then restore between the oxidation and reduction.

3.5. Reproducibility and stability studies

The reproducibility and stability of the modified electrode were evaluated in these sensing studies. The relative standard deviation (RSD) for five measurements was 2.3%, suggesting acceptable repeatability and precision. Moreover, the stability of the CD/r-GO/GCE was checked, shown in Fig. S3.† The response of the modified electrode to 0.2 mM dihydroxybenzene isomer solution only decreased 2.63% of its initial response signal after being stored for 2 weeks, indicating the good stability of the sensor. Moreover, some common interferents for the

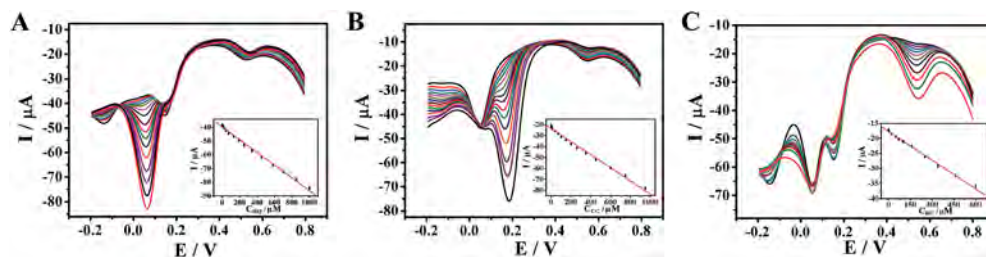


Fig. 6 DPVs of HQ concentrations: 0, 0.2 μM , 1.0 μM , 10 μM , 20 μM , 40 μM , 70 μM , 130 μM , 190 μM , 250 μM , 340 μM , 450 μM , 580 μM , 700 μM , 850 μM and 1000 μM . (B) DPVs of CC concentrations: 0, 1.0 μM , 5.0 μM , 10.0 μM , 40 μM , 70 μM , 100 μM , 150 μM , 200 μM , 260 μM , 350 μM , 450 μM , 600 μM , 750 μM and 900 μM . (C) DPVs of RC concentrations: 0, 5.0 μM , 20 μM , 50 μM , 70 μM , 100 μM , 160 μM , 250 μM , 340 μM , 460 μM and 600 μM at the CD/r-GO/GCE in the presence of other two interfering substances (concentration 0.2 μM).

Table 1 Comparison of different electrochemical sensors for the determination of dihydroxybenzene isomers

Electrode	Linear (μM)			Detection limit (μM)			Ref.
	HQ	CC	RC	HQ	CC	RC	
Graphene-chitosan/GCE	1.0–400	1.0–550	1.0–300	0.75	0.75	0.75	4
CNF/GCE	6.0–200	2.0–200	—	0.25	0.1	—	5
Pt/ZrO ₂ -rGO/GCE	1.0–1000	1.0–400	—	0.4	0.4	—	11
r-GO-MWNT/GCE	8.0–391	5.5–540	—	2.6	1.8	—	22
WS ₂ -graphene/GCE	1.0–100	1.0–100	1.0–100	0.1	0.2	0.1	23
EG/GCE	6–200	1–200	—	0.2	0.1	—	40
Graphene/GCE	1–500	1–500	—	0.015	0.01	—	43
CD/r-GO/GCE	0.5–1000	1.0–950	5.0–600	0.17	0.28	1.0	This work

Table 2 Results of the determination of dihydroxybenzene isomers in real samples

Samples	Original (μM)			Added (μM)			Found (μM)			Recovery (%)		
	HQ	CC	RC	HQ	CC	RC	HQ	CC	RC	HQ	CC	RC
Tap water	0	0	0	100	100	100	100.6 \pm 0.5	101.3 \pm 0.4	99.2 \pm 0.9	100.9	101.5	98.7
River water	0	0	0	200	200	200	199.6 \pm 0.5	201.3 \pm 0.4	198.8 \pm 0.9	99.7	100.8	99.2
Industrial sewage	230 \pm 1.9	85 \pm 1.3	15 \pm 1.1	100	100	100	328.2 \pm 2.6	185.9 \pm 2.4	115.8 \pm 2.1	99.1	101.2	101.7
				200	200	200	427.8 \pm 2.6	286.3 \pm 2.7	216.4 \pm 3.9	99.2	100.8	101.6

simultaneous determination of HQ, CC and RC were also investigated, such as MgCl₂, NaCl, K₂SO₄ solutions (100 fold), phenol, nitrophenol and glucose solutions (50 fold). The oxidation peak potential and current of HQ, CC and RC were observed almost constantly in the presence of all interferents. Thus, the results indicated that the CD/r-GO/GCE exhibited good selectivity for the detection of dihydroxybenzene isomers.

3.6. Application of the method for the analysis of samples

A comparison of the proposed method with other electrochemical methods reported for the determination is shown in Table 1.⁴³ A wider linear range and lower detection limit of the CD/r-GO/GCE sensor for the simultaneous detection of HQ, CC and RC were observed. For further evaluation of the applicability of the method, tap water, local river water and industrial sewage samples were used for quantitative analysis after filtering with a cellulose membrane filter (pore size 0.25 μm) several times. Then, 5 mL of the real samples were diluted to 10

mL with 0.1 mM PBS solutions. The results are shown in Table 2. The recovery of the real samples ranged between 98.7% and 101.7% ($n = 6$). The results indicated the practical applicability of the CDs/r-GO/GCE for simultaneous determination of HQ, CC and RC in real water samples.

4. Conclusions

In summary, the CD/r-GO composite was designed and constructed as electrode materials. The support matrix r-GO straightforwardly combined with CDs was used as an electrochemical sensor for the simultaneous determination of HQ, CC and RC for the first time. The performance of the electrode improved greatly compared with that of the electrode modified by r-GO or CDs alone because of its unique chemical and electrochemical properties and its synergetic effect. Detection limits for HQ, CC and RC were 0.17 μM , 0.28 μM and 1.0 μM ($S/N = 3$), respectively. Excellent reproducibility and stability in practical

water samples show that this novel composite can provide a promising platform for the quantitative detection of HQ, CC and RC at the micromole level for real samples.

Acknowledgements

This project was supported by Fujian Province Natural Science Foundation (2012D136), the Science and Technology Foundation of Fujian Provincial Bureau Quality and Technical Supervision (no. FJQI 2013108), National Undergraduate Innovative Training Program (201410402002).

References

- 1 M. Narmadha, M. Noel and V. Suryanarayanan, *J. Electroanal. Chem.*, 2011, **655**, 103.
- 2 S. Palanisamy, C. Karuppiah, S. M. Chen, K. Muthupandi, R. Emmanuel, P. Prakash, M. S. Elshikh, M. A. Ali and F. M. A. Al-Hemaid, *Electroanalysis*, 2015, **27**, 1.
- 3 J. Qu, Y. Wang, Y. Dong, Z. Zhu and H. Xing, *Anal. Methods*, 2015, **7**, 260.
- 4 H. Yin, Q. Zhang, Y. Zhou, Q. Ma, T. Liu, L. Zhu and S. Ai, *Electrochim. Acta*, 2011, **56**, 2748.
- 5 C. Zhang, L. Zeng, X. Zhu, C. Yu, X. Zuo, X. Xiao and J. Nan, *Anal. Methods*, 2013, **357**, 2203.
- 6 G. Marrubini, E. Calleri, T. Coccini, A. F. Castoldi and L. Manzo, *Chromatographia*, 2005, **62**, 25.
- 7 P. S. Selvan, R. Gopinath, V. S. Saravanan, N. Gopal, S. A. Kumar and K. Periyasamy, *Asian J. Chem.*, 2007, **19**, 1004.
- 8 P. Nagaraja, R. A. Vasantha and K. R. Sunitha, *Talanta*, 2001, **55**, 1039.
- 9 P. R. Dalmaso, M. L. Pedano and G. A. Rivas, *Sens. Actuators, B*, 2012, **173**, 732.
- 10 A. Navaee, A. Salimi and H. Teymourian, *Biosens. Bioelectron.*, 2012, **31**, 205.
- 11 A. T. E. Vilian, S. M. Chen, L. H. Huang, M. A. Ali and F. AlHemaid, *Electrochim. Acta*, 2014, **125**, 503.
- 12 S. Wu, Q. He, C. Tan, Y. Wang and H. Zhang, *Small*, 2013, **9**, 1160.
- 13 R. K. Joshi, P. Carbone, F. C. Wang, V. G. Kravets, Y. Su, I. V. Grigorieva, H. A. Wu, A. K. Geim and R. R. Nair, *Science*, 2014, **343**, 752.
- 14 K. P. Loh, Q. Bao, P. K. Ang and J. Yang, *J. Mater. Chem.*, 2010, **20**, 2277.
- 15 R. Song, W. Feng, C. A. Jimenez-Cruz, B. Wang and W. Jiang, *RSC Adv.*, 2015, **5**, 274.
- 16 S. Bai, J. Ge, L. Wang, M. Gong, M. Deng, Q. Kong, L. Song, J. Jiang, Q. Zhang, Y. Luo, Y. Xie and Y. Xiong, *Adv. Mater.*, 2014, **32**, 5689.
- 17 F. H. L. Koppens, T. Mueller, P. Avouris, A. C. Ferrari, M. S. Vitiello and M. Polini, *Nat. Nanotechnol.*, 2014, **9**, 780.
- 18 F. Meng, X. Zhang, B. Xu, S. Yue, H. Guo and Y. Luo, *J. Mater. Chem.*, 2011, **21**, 18537.
- 19 A. N. Aleshin, I. P. Shcherbakov, A. S. Komolov, V. N. Petrov and I. N. Trapeznikova, *Org. Electron.*, 2015, **16**, 186.
- 20 S. Hu, W. Zhang, J. Zheng, J. Shi, Z. Lin, L. Zhong, G. Cai, C. Wei, H. Zhang and A. Hao, *RSC Adv.*, 2015, **5**, 18615.
- 21 X. Ma, Z. Liu, C. Qiu, T. Chen and H. Ma, *Microchim. Acta*, 2013, **180**, 461.
- 22 F. Hu, S. Chen, C. Wang, R. Yuan, D. Yuan and C. Wang, *Anal. Chim. Acta*, 2012, **724**, 40.
- 23 K. J. Huang, L. Wang, Y. J. Liu, T. Gan, Y. M. Liu, L. L. Wang and Y. Fan, *Electrochim. Acta*, 2013, **107**, 379.
- 24 Q. Liu, B. Guo, Z. Rao, B. Zhang and J. R. Gong, *Nano Lett.*, 2013, **13**, 2436.
- 25 H. Li, X. He, Y. Liu, H. Huang, S. Lian, S. T. Lee and Z. Kang, *Carbon*, 2011, **49**, 605.
- 26 H. Li, Z. Kang, Y. Liu and S. T. Lee, *J. Mater. Chem.*, 2012, **22**, 24230.
- 27 C. G. Joaquim, D. S. Esteves and M. R. G. Helena, *Trends Anal. Chem.*, 2011, **30**, 1327.
- 28 S. Qu, X. Wang, Q. Lu, X. Liu and L. Wang, *Angew. Chem., Int. Ed.*, 2012, **51**, 12215.
- 29 J. C. G. Esteves da Silva and H. M. R. Goncalves, *TrAC, Trends Anal. Chem.*, 2011, **30**, 1327.
- 30 W. Kwon and S. W. Rhee, *Chem. Commun.*, 2012, **48**, 5256.
- 31 Y. Li, Y. Zhong, Y. Zhang, W. Weng and S. Li, *Sens. Actuators, B*, 2015, **206**, 735.
- 32 W. S. Hummers and R. E. Offeman, *J. Am. Chem. Soc.*, 1958, **80**, 1339.
- 33 X. Kang, J. Wang, H. Wu, I. A. Aksay, J. Liu and Y. Lin, *Biosens. Bioelectron.*, 2009, **25**, 901.
- 34 G. Wang, B. Wang, J. Park, J. Yang, X. Shen and J. Yao, *Carbon*, 2009, **47**, 68.
- 35 Q. Liang, W. Ma, Y. Shi, Z. Li and X. Yang, *Carbon*, 2013, **60**, 421.
- 36 C. Zhu, J. Zhai and S. Dong, *Chem. Commun.*, 2012, **48**, 9367.
- 37 P. V. Kumar, N. M. Bardhan, S. Tongay, J. Wu, A. M. Belcher and J. C. Grossman, *Nat. Chem.*, 2014, **6**, 151.
- 38 S. N. Baker and G. A. Baker, Luminescent Carbon Nanodots: Emergent Nanolights, *Angew. Chem., Int. Ed.*, 2010, **49**, 6726.
- 39 Q. Li, B. Guo, J. Yu, J. Ran, B. Zhang, H. Yan and J. R. Gong, *J. Am. Chem. Soc.*, 2011, **133**, 10878.
- 40 H. Du, J. Ye, J. Zhang, X. Huang and C. Yu, *J. Electroanal. Chem.*, 2011, **650**, 209.
- 41 Y. Hu, F. Li, X. Bai, D. Li, S. Hua, K. Wang and L. Niu, *Chem. Commun.*, 2011, **47**, 1743.
- 42 X. Feng, W. Gao, S. Zhou, H. Shi, H. Huang and W. Song, *Anal. Chim. Acta*, 2013, **805**, 36.
- 43 L. Chen, Y. Tang, K. Wang, C. Liu and S. Luo, *Electrochem. Commun.*, 2011, **13**, 133.